

# ENHANCED OXIDATION RESISTANCE AND MICROHARDNESS OF NI-YSZ COMPOSITES VIA THE FORGING IN AIR

O.Yu. Kurapova<sup>1,2</sup>, E.N. Solovyeva<sup>1,3</sup>, I.V. Lomakin<sup>2</sup>, V.M. Ushakov<sup>3</sup>,  
I.Yu. Archakov<sup>1,4</sup> and V.G. Konakov<sup>1,2,3</sup>

<sup>1</sup>Peter the Great St. Petersburg Polytechnic University, St. Petersburg 195251, Russia

<sup>2</sup>St. Petersburg State University, Universitetskaya emb. 7/9, St. Petersburg, 199034, Russia

<sup>3</sup>Glass and Ceramics Ltd., 9 Linia V.O., 20, St. Petersburg, 199004, Russia

<sup>4</sup>Institute for Problems of Mechanical Engineering, Russian Academy of Sciences, St. Petersburg, 199178, Russia

Received: May 25, 2018

**Abstract.** Nickel-ceramics composites are very promising materials for various industrial applications. Significant progress was achieved in the field of composite nickel-ceramic coatings development. However, in case of bulk nickel-ceramics composites the available information is quite insufficient. In this study the effect of forging on the microstructure, oxidation resistance, and microhardness of Ni-8Y<sub>2</sub>O<sub>3</sub>-92ZrO<sub>2</sub> (Ni-YSZ) composites was revealed. Nickel-YSZ composites were manufactured by powder metallurgy technique with following vacuum annealing at 1250 °C; in addition, forging at 1000 °C was applied. Oxidation behavior was studied by thermogravimetry in air. The microstructure of the composites was investigated via SEM, XRD, and EBSD analysis. It was shown that forged composites do not undergo oxidation in the temperature range 20-950 °C. Forged Ni-YSZ composites exhibited improved Vickers hardness (HV) compared to bulk nickel.

## 1. INTRODUCTION

Due to high ductility and sufficient strength, nickel and its alloys are widely used for various industrial applications [1-3]. However, rather low oxidation resistance at elevated temperatures remains the main disadvantage of pure Ni. Along with complex alloys design, the development of novel nickel based materials is a promising way for the significant improvement of the oxidation resistance and mechanical characteristics of nickel matrix [4-7]. The use of various ceramic nanoparticles (oxides, borides, nitrides, carbides, etc.) as additives to the metallic nickel is regarded to be an efficient way of mechanical characteristics improvement coupled with oxidation resistance enhancement. As it is mentioned

in [8] rare oxides are widely used for novel Ni-based alloy and Fe-based alloy coatings manufacturing by laser cladding, chemical deposition, electroplating technique. Recently, "Ni-nanoSm<sub>2</sub>O<sub>3</sub>", and "Ni-nanoCeO<sub>2</sub>" composite coatings with enhanced microhardness, wear resistance, and electrochemical corrosion resistance have been fabricated via laser deposition technique [8]. The greatest properties improvement was reached upon 1.5% nano CeO<sub>2</sub> and Sm<sub>2</sub>O<sub>3</sub> powders introduction. Binary "Ni-SiC" and "Ni-Al<sub>2</sub>O<sub>3</sub>" composite coatings possessing high electrochemical corrosion resistance, improved mechanical, and tribological properties were manufactured via wet chemical techniques in [9,10]. The oxidation resistance of Ni-SiC coating was in-

Corresponding author: O.Yu. Kurapova, e-mail: o.y.kurapova@spbu.ru

vestigated in [11] at 1000 °C. It was shown that the 94Ni-6SiC (wt.%) nanocomposite coating exhibited a superior oxidation resistance compared with the pure Ni film due to the formation of SiO<sub>2</sub> oxide particles along grain boundaries; the oxidation mechanism was discussed in detail. In [12] it was shown that the incorporation of Al<sub>2</sub>O<sub>3</sub> particles also results in about twice decreased weight gain of Ni- Al<sub>2</sub>O<sub>3</sub> composites at 900 °C comparing to pure Ni film, i.e. the improved oxidation resistance. The effect of synthesis technique was also highlighted in this work.

In our recent work [13] oxidation behavior of bulk Ni-Y<sub>2</sub>O<sub>3</sub>-92ZrO<sub>2</sub> (YSZ) composites was investigated at 800 and 900 °C. It was shown that a 2-5 wt.% YSZ addition enhances the oxidation resistance of bulk nickel based composites in 2-3 times comparing to bulk nickel which is due NiO growth in the pores. In case of bulk nickel-ceramic composites, the intensive oxidation often takes place due to its high porosity, i.e. large surface area where air oxygen contacts the material. Forging is one of the efficient ways to diminish porosity of metallic materials. The decreased oxidation of bulk nickel based composites after forging is expected. Thus, the goal of the work was the investigation of the forging effect on the microstructure, oxidation resistance, and Vickers hardness of (100-x)Ni - xYSZ composites (x = 0.1 and 1 wt.%).

## 2. EXPERIMENTAL

### 2.1. Composites manufacturing

In order to obtain 99.9Ni-0.1YSZ and 99Ni-1YSZ (wt.%, here and after Specimens 1 and 2, respectively) composite specimens, preliminary sieved commercial fine-grained nickel powder, see [13,14] for details, and nanosized yttria stabilized zirconia powder (8Y<sub>2</sub>O<sub>3</sub>-92ZrO<sub>2</sub>, mol.%, 8YSZ) were used as starting materials. Yttria stabilized zirconia was obtained by reversed co-precipitation technique with following freeze-drying and calcination at 700 °C [15]. Powders were mixed in the defined proportions. Then the composite specimens were fabricated by modified powder metallurgy technique recently reported by authors in [13]. The mixtures were milled in a planetary ball mill (Pulverisette 6, Fritzch) at 450 rpm for 6 hours. Mechanically activated powders were cold pressed into pellets of 30 mm in the diameter and 15 mm in height under the pressure of 15 tons/cm<sup>2</sup> at room temperature. As a result, tablet-like specimens were fabricated. Specimens were annealed at 1250 °C for 1 hour (heating rate 10 °C/min, cooling with the furnace ~ 6 hours down to 500

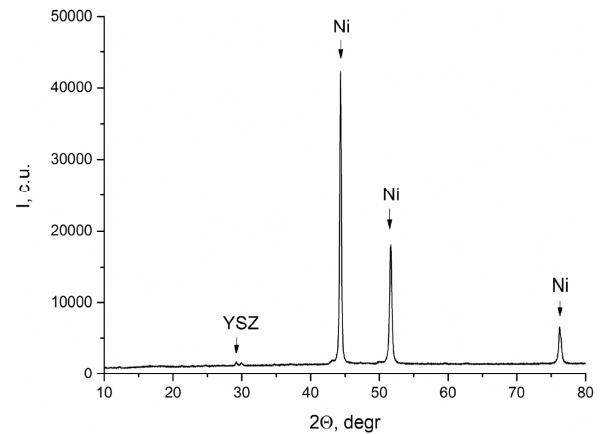
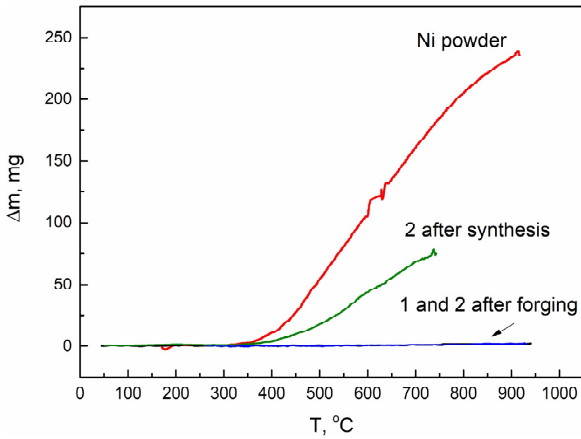


Fig.1. XRD pattern for specimen 2 after forging.

°C) in a vacuum furnace with the residual pressure less than 0.003 atm. In order to diminish the porosity, specimens underwent uniform forging at 1000 °C in air.

### 2.2. Analysis

Oxidation resistance of specimens was revealed via TG analysis (derivatograph MOM-3, Hungary). Phase composition of Specimens before and after oxidation was determined via X-Ray diffraction analysis (XRD, Shimadzu XRD-6000). X-ray diffraction patterns analysis for the polycrystalline samples has been performed in air at room temperature using Cu K $\alpha$  radiation,  $\lambda = 1.54 \text{ \AA}$ . Microstructure of samples surface after the synthesis was investigated by scanning electron microscopy (SEM, Hitachi S-3400N with the equipment for energy dispersive analysis, EDX). Electron back scattering diffraction (EBSD) was used to characterize sample microstructure. For EBSD measurements, a Hitachi S-3400N scanning electron microscope equipped with Oxford HKL Nordlys EBSD detector was used. Operating conditions were as follows: accelerating voltage 20 kV, beam current 1 nA. Patterns of backscattered electrons (EBSP) were acquired from rectangular grid with the step size of 0.3  $\mu\text{m}$  (0.1  $\mu\text{m}$ ) for 46  $\mu\text{sec}$  per one EBSP acquisition during mapping. Oxford Instruments Aztec HKL analysis software was used to identify the crystal orientation from the Kikuchi pattern in automatic mode, the crystal structure of Ni metal was used to estimate the grain size in the composites. Vickers hardness (HV) was determined at the load of 0.5 kg applied for 15 seconds (Shimadzu HMV-G21, diamond pyramid shaped indenter). The data for each Specimen were averaged over 25 tests.



**Fig.2.** TG curves obtained for specimens 1 and 2 before after forging and pure nickel powder.

### 3. RESULTS AND DISCUSSION

XRD patterns of Specimen 2 composite after forging are presented in Fig. 1. As it is seen from Fig. 1, metallic nickel is the main phase in Specimen 2. Small peak at  $2\theta=29.5^\circ$  corresponds to yttria stabilized zirconia solid solution. No reflexes attributed to nickel oxide ( $\text{NiO}$ ,  $2\theta \sim 37, 43, 62.5^\circ$  [16]) were observed indicating that no oxidation takes place during forging at  $1000^\circ\text{C}$  in air. Similar results were obtained for the composite containing 0.1 wt.% YSZ. The only difference is that Specimen 1 pattern is quite similar to pure Ni one since the amount of YSZ phase is below the detection limit of XRD analysis.

Termogravimetry was performed for Specimens 1 and 2 before and after forging in order to investigate the oxidation behavior in the range of 20-1000  $^\circ\text{C}$  in air. Corresponding TG curves are presented in Fig. 2 together with the data for pure nickel powder used as a starting material. It should be noted that it was impossible to forge the pure nickel specimen, since the resulted forged specimen turned to be too brittle. So, TG and microhardness data were not obtained for that specimen.

From Fig. 2 it is seen that temperature behavior of pure Ni powder is characterized by readily oxida-

tion to  $\text{NiO}$  in air. It should be taken into consideration that a high specific area of Ni powder contributes significantly to the to the oxidation rate. Namely, weight increase of pure nickel powder is 237 mg/g which corresponds to  $\sim 80\%$  of oxidized nickel (see TG curve for pure Ni). Notable oxidation of untreated specimen 2 is observed as well. At the same time, almost no change in weight is observed on TG curves of Specimens 1 and 2 after forging upon heating. At  $\sim 950^\circ\text{C}$ , the weight gain of for Specimens 1 and 2 after forging is 2.3 and 2.5 mg/g, respectively. So, one can conclude that no oxidation takes place in the composites in all the experimental temperature range. In order to investigate the oxidation resistance of the composites at the long-time exposure, Specimens 1 and 2 were thermally treated at  $900^\circ\text{C}$  for 24 hours. For both specimens no notable weight gain was detected indicating the negligible oxidation.

The data on specimen microhardness are presented in Table 1 comparing to the data reported [13] on composites microhardness after synthesis. It should be noted that pure nickel turned to be unable to forge because of material brittleness.

Let us discuss these results in more detail. The addition of 1 wt.% YSZ to pure nickel results in  $\sim 30\%$  microhardness increase. However, it results also in the significant experimental error. Forging of Specimen 2 results in rather close microhardness values, i.e.  $79.18 \pm 22.94$  and  $71.37 \pm 7.17$  HV before and after forging, respectively (see Table 1). Notable, that forging leads to the experimental error decrease to  $\sim 10\%$  indicating more uniform structure of Specimen 2 after forging. Specimen 1 after forging is characterized by the highest microhardness value of  $123.2 \pm 6.77$  HV, which is twice more than the value of Specimen of pure Ni. The remarkable oxidation resistance and high microhardness values observed are, likely, due to the refined microstructure of composite 1 after the treatment by forging. The microstructure of the 99Ni-1YSZ composite (Specimen 2) after the synthesis and oxidation at 800 and  $900^\circ\text{C}$  was discussed in the recent works of the au-

**Table 1.** Mechanical properties of Ni-YSZ composites before and after forging.

| Specimen | wt.% YSZ | Microhardness, HV<br>No forging<br>Data from [13] | Microhardness, HV<br>No forging, data from [13] |
|----------|----------|---|---|
| 3        | 0        | $60.06 \pm 2.74$                                  | -   |
| 1        | 0.1      | -   | $123.2 \pm 6.77$                                |
| 2        | 1        | $79.18 \pm 22,94$                                 | $71.37 \pm 7.17$                                |

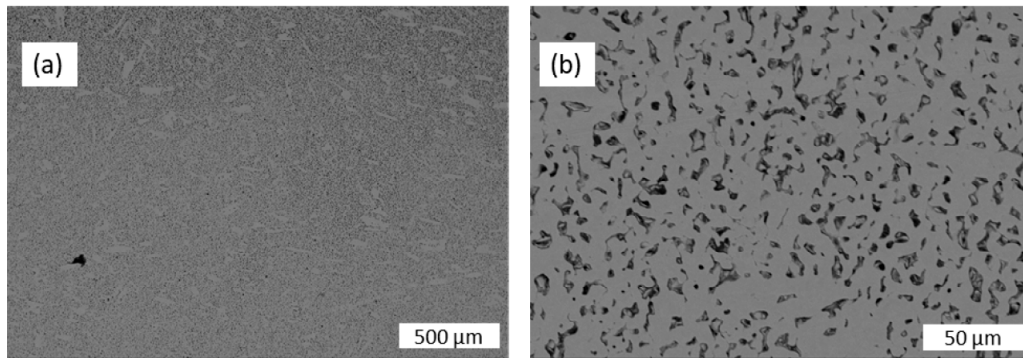


**Fig. 3.** SEM microphotographs of the Specimen 1 after forging. Magnification (a) x50, (b) x500.

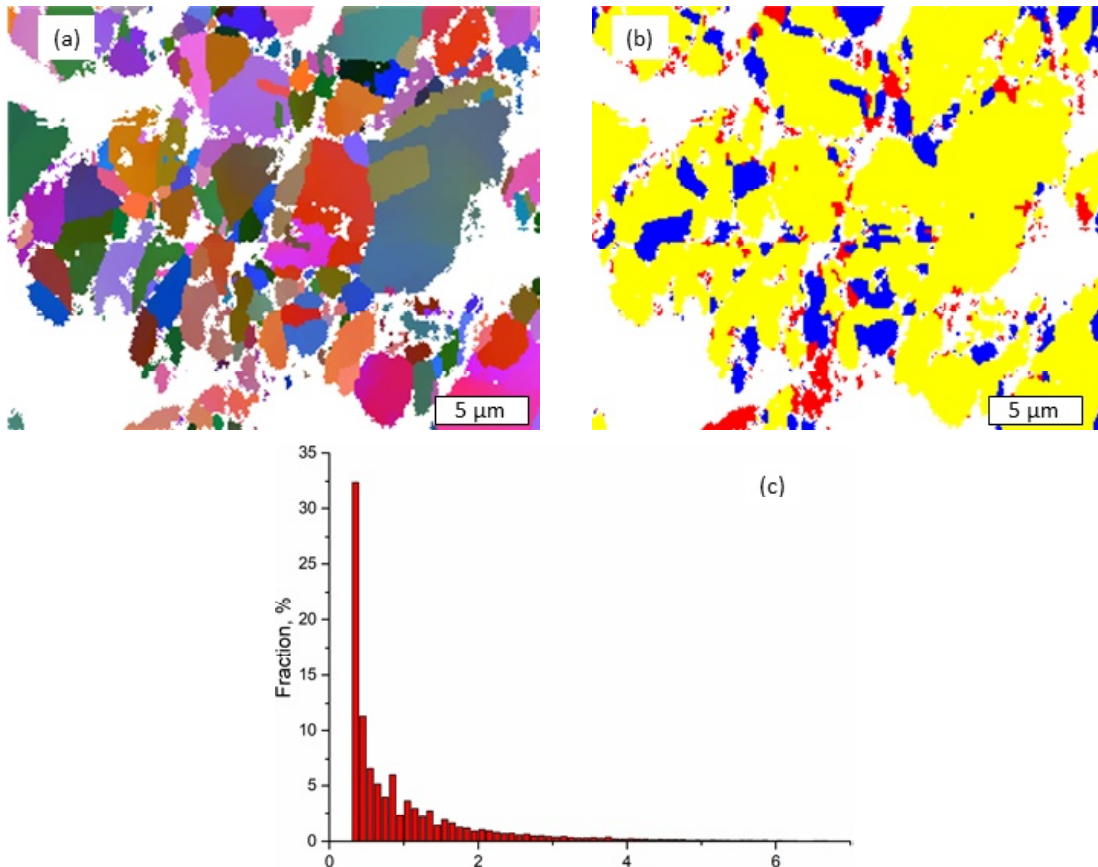


**Fig. 4.** (a) EBSD map of Specimen 1 (b) IPF map obtained from EBSD data (c) grain size distribution in the specimen.

thors [13,15]. In particular, it was shown that the addition of 1-2 wt.% of YSZ reduces sample porosity and slightly enhances the roughness of composite comparing to pure nickel specimen. Oxidation takes place simultaneously with grain coarsening and pore size redistribution. Since specimen 1 shows remarkably different behavior further the microstructural features of the 99.9Ni-0.1YSZ will be discussed. The surface of the composite specimen 1 (99.9Ni-0.11YSZ, wt.%) after forging is shown in Fig. 3.

From the Fig. 3a it is seen that surface of the specimen is rather uniform and smooth. Residual

amount of the pores and defects is observed. Under higher magnification (x500, Fig. 3b) mostly closed porosity can be identified. No micropores are observed on the surface of Specimen 1. Thus, comparing to SEM data of [15] one can conclude that forging leads to porosity and surface roughness decrease. According to EDX analysis, the YSZ additive is homogeneously dispersed in Specimens 1 and 2 after forging. Chemical composition is in accordance with the initial composition before the synthesis (brutto composition).

In order to investigate the effect of forging on the grain refinement, grain redistribution, and structure

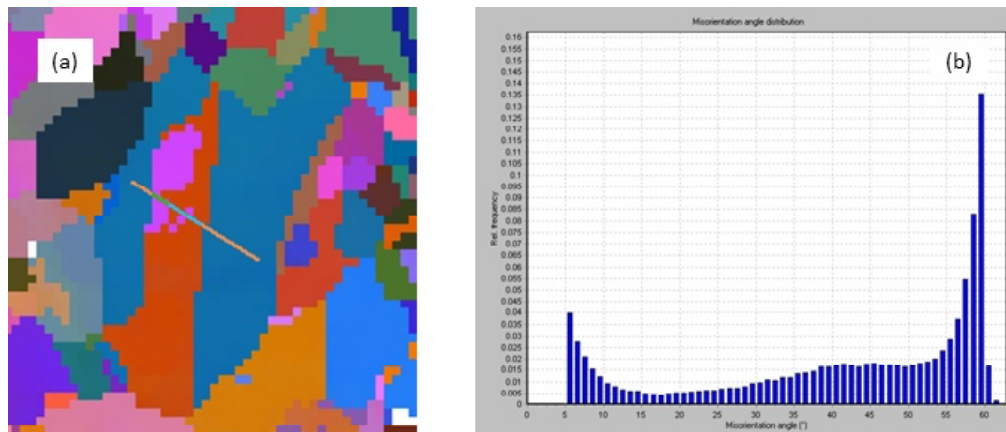


**Fig. 5.** EBSD data of Specimen 2 (a) IPF map of twinned grains (b) grain misorientation angles distribution.

defectiveness of the composites EBSD analysis was performed for Specimen 1. Fig. 4 shows the IPF maps obtained by EBSD.

As it seen from EBSD map, presented in Fig. 4a, grains after forging are mostly micron-sized corresponding to coarse grained structure (CG). Estimated size of the grains is  $\sim 2\text{-}10\ \mu\text{m}$ . Their size is comparable to average pores size. However significant amount of ultrafine grains (UFG) present in Specimen 1 structure, likely being a result of allied deformation upon forging. Indeed, mean grain diameter is  $1.06\ \mu\text{m}$  (see Fig. 4c). The maximum of grain fraction corresponds to  $0.35\ \mu\text{m}$ . As it is seen from IPF map in Fig 4b, UFG correspond to either recrystallized or deformed grains. The fraction of the deformed grains, calculated from IPF map data, is about  $\sim 53\%$ . Coarse grains are surrounded by the deformed and recrystallized grains. Recrystallization and deformation, likely, take place during forging. UFG fill partially pores, which, possibly, causes microhardness enhancement. Besides, the significant amount of twins is present in composite structure which is most likely a result of recrystallization of nickel grains [17]. Typical twin is presented in Fig. 5a. The misorientation angle corresponds to  $60^\circ$ , that characterizes the twinning in FCC (face cubic centered) lattice (see misorientation angle distribution in Fig. 5b).

Summarizing the results obtained, one can see that the introduction of  $0.1\ \text{wt.}\%$  YSZ to Ni as well as treatment by forging results in the remarkable enhancement of the oxidation resistance and microhardness which is due to porosity reduction of the material.

#### 4. CONCLUSIONS

A novel technique for the fabrication of the nickel-ceramic composites with the enhanced

microhardness and oxidation resistance was suggested including milling in a planetary mill, vacuum annealing  $1250\ ^\circ\text{C}$  and forging at  $1000\ ^\circ\text{C}$  is suggested. No notable oxidation was observed in case of forged nickel-YSZ composites up to  $\sim 950\ ^\circ\text{C}$ . It was shown that forging causes significant Vickers hardness improvement of  $99.9\text{Ni-}0.1\text{YSZ}$  (wt.%) composite comparing pure nickel specimen. Using SEM and EBSD, it was proved that the observed oxidation resistance and Vickers hardness improvement is due to overall porosity and surface roughness decrease.

#### ACKNOWLEDGEMENTS

This research work was supported by Ministry of Education and Science of Russian Federation, Zadanie 16.3483.2017/PCh. SEM and EBSD data were obtained at the Research park of St. Petersburg State University Center for Geo-Environmental Research and Modeling (GEOMODEL). Authors are grateful to Dr. Ilya Gusev for conducting the forging experiment.

#### REFERENCES

- [1] E. Breval // *Composites Part B: Engineering* **5** (1995) 1127.
- [2] S.R. Yu, Y. Liu, W. Li, J.A. Liu and D.S. Yuan // *Composites Part B: Engineering* **43** (2012) 1070.
- [3] V. Provenzano and R. L. Holtz // *Mat. Sci. Eng.: A* **204** (1995) 125.
- [4] R. Darolia // *Journal of Metals* **43** (1991) 44.
- [5] A. Mortensen, J.R. Cornie and M.C. Flemings // *J. Met.* **40** (1988) 12.
- [6] P.M. Ajayan, L.S. Schadler and P.V. Braun, *Nanocomposite science and technology* (John Wiley&Sons, 2006).

- [7] G. Zauthoff and B. Tsoimer, *Patent RU 2148671*, 10.05.2000.
- [8] S. Zhang, M. Li, J. H. Yoon, T. Y. Cho, C. G. Lee and Y. He // *Applied Surface Science* **254** (2008) 7446.
- [9] Y S. Huang, X.T. Zeng, X.F. Hu and F.M. Liu // *Electrochimica Acta* **49** (2004) 4313.
- [10] N. S. Qu, K. C. Chan and D. Zhu // *Scripta Materialia* **50** (2004)1131.
- [11] Y. B. Zhou and Y. Z. Ding // *Transactions of Nonferrous Metals Society of China* **17** (2007) 925.
- [12] Q. Feng, T. Li, H. Teng, X. Zhang, Y. Zhang, C. Liu, and J. Jin // *Surface and Coatings Technology* **202** (2008) 4137.
- [13] O. Y. Kurapova, I. V. Lomakin, E. N. Solovieva, I. Y. Archakov and V. G. Konakov // *Rev. Adv. Mater. Sci.* **52** (2017) 99.
- [14] V.G. Konakov, E.N. Solovyeva, O.Yu. Kurapova, N.N. Novik, M.M. Pivovarov and I.Yu. Archakov // *Materials Physics and Mechanics* **24** (2015) 340.
- [15] V.G. Konakov, I.A. Ovid'ko, E.N. Solovyeva, O.Yu. Kurapova, N.N. Novik and M.M. Pivovarov // *Materials Physics and Mechanics* **24** (2015) 331.
- [16] PDF (powder diffraction file) database, release 2, 2012.
- [17] V. Randle, P. R. Rios and Y. Hu // *Scripta Materialia* **58** (2008) 130.